Acta Biomaterialia 25 (2015) 253–267

Contents lists available at ScienceDirect

Acta Biomaterialia

journal homepage: www.elsevier.com/locate/actabiomat

The effect of Young's modulus on the neuronal differentiation of mouse embryonic stem cells

Shahzad Ali [a], Ivan B. Wall [a], Chris Mason [a], Andrew E. Pelling [b], Farlan S. Veraitch [a,*]

[a] Advanced Centre for Biochemical Engineering, University College London, Torrington Place, London WC1E 7JE, United Kingdom
[b] The Pelling Lab, University of Ottawa, Center for Interdisciplinary Nanophysics, MacDonald Hall (MCD), 150 Louis Pasteur, Ottawa, ON K1N6N5, Canada

ARTICLE INFO

Article history:
Received 5 November 2014
Received in revised form 27 May 2015
Accepted 5 July 2015
Available online 6 July 2015

Keywords:
Young's modulus
Embryonic stem cells
Atomic force microscopy
Neuronal differentiation

ABSTRACT

There is substantial evidence that cells produce a diverse response to changes in ECM stiffness depending on their identity. Our aim was to understand how stiffness impacts neuronal differentiation of embryonic stem cells (ESC's), and how this varies at three specific stages of the differentiation process. In this investigation, three effects of stiffness on cells were considered; attachment, expansion and phenotypic changes during differentiation. Stiffness was varied from 2 kPa to 18 kPa to finally 35 kPa. Attachment was found to decrease with increasing stiffness for both ESC's (with a 95% decrease on 35 kPa compared to 2 kPa) and neural precursors (with a 83% decrease on 35 kPa). The attachment of immature neurons was unaffected by stiffness. Expansion was independent of stiffness for all cell types, implying that the proliferation of cells during this differentiation process was independent of Young's modulus. Stiffness had no effect upon phenotypic changes during differentiation for mESC's and neural precursors. 2 kPa increased the proportion of cells that differentiated from immature into mature neurons. Taken together our findings imply that the impact of Young's modulus on attachment diminishes as neuronal cells become more mature. Conversely, the impact of Young's modulus on changes in phenotype increased as cells became more mature.

1. Introduction

Embryonic stem (ES) cells, derived from the early mammalian embryo are unique in their ability to both self renew indefinitely *in vitro* [1] as well as differentiate into cells from any of the 3 germ layers (endoderm, mesoderm and ectoderm) and thus form any tissue within the body [2]. As a result of these two properties, there has been much interest generated in potential therapeutic applications for embryonic stem cells, including treatments for Parkinson's disease [3–6], diabetes [7–9] and cardiovascular disease [10–14]. Despite promising early studies in animals, production of the large quantities of cells required for therapeutic use in humans will require a substantial improvement on the current cell processing technology [15,16].

One approach to improve the efficiency of stem cell processes has been to investigate the role of the mechanical microenvironment. This includes factors such as cyclic strain [17], shear from fluid flow [18] and extracellular matrix elasticity [19–21] which have all been shown to be key regulators of stem cell differentiation. Culturing cells on a matrix elasticity similar to that of the *in vivo* microenvironment has in particular shown to have a profound effect on the behaviour of somatic cells, including increased beating in cardiomyocytes [22], increased spreading of fibroblasts [23] and direction of differentiation in myoblasts [24].

A seminal study by Engler et al. in 2006 [19] showed that culturing mesenchymal stem cells on polyacrylamide gels with a Young's modulus associated with a specific tissue type (such as brain, muscle or cross-linked collagen in osteoids) promoted directed differentiation into that lineage. In an investigation into the effect of stiffness on ES cell differentiation, Evans et al. [25] showed that osteogenic gene expression increased when mESC's were differentiated on stiff PDMS materials, whose elasticity corresponded with that of bone. There has been little study as of yet as to how Young's modulus affects the formation of neuronal precursors and immature neurons from mESC's. There have however been many attempts at studying the effect of stiffness on primary cultures of mixed cortical neurons [26], mixed hippocampal neurons [27], embryonic rat spinal cord [28] or neural stem cells [29,30]. In the case of mixed cortical neurons [26], 80% of cells were positive for β-III tubulin on soft, 100 Pa polyacrylamide gels compared to 45% on stiffer, 9 kPa polyacrylamide gels. Neuronal adhesion did not vary between materials in this study. Jiang and colleagues [28] showed a similar finding using mixed embryonic rat spinal cord,

* Corresponding author.
E-mail address: f.veraitch@ucl.ac.uk (F.S. Veraitch).

http://dx.doi.org/10.1016/j.actbio.2015.07.008
1742-7061/

where MAP2-positive neuronal adhesion did not vary with Young's modulus from 0.3 kPa to 27 kPa. In that study, both the adhesion and maturation of immature astrocytes increased with an increase in Young's modulus from 0.3 kPa to 27 kPa. The number of mixed hippocampal neurons (per cm^2) found on polyacrylamide gels at 24 h post-attachment also did not vary [27] with Young's modulus from 2 kPa to 18 kPa. In the case of neural stem cells, β-III tubulin gene expression peaked on soft materials (200 Pa in Banerjee et al.'s study on 3D hydrogels [29]; between 500 Pa and 1 kPa in Saha et al.'s study on 2D gels [30]).

In most of the aforementioned studies [26,29,30], soft materials in the range of 0.1 to 1 kPa, corresponding to the elasticity range of tissues found in central nervous system and brain [31], generally lead to higher expression of markers such as βIII tubulin and MAP2, which are early markers for maturation into cells with neuronal morphology [32].

Adhesion of primary neuronal and neural stem cell cultures was unaffected by Young's modulus in most cases [26–28,30]. In Flanagan et al.'s study, soft (50 Pa) polyacrylamide gels were found to increase neurite branching [33] in comparison to stiffer (550 Pa) gels. This is an important consideration when introducing reparative cells into diseased areas, where the mechanical microenvironment may be considerably different to that of healthy tissue, as well as *in vitro* conditions. For example, glial scarring, associated with spinal cord damage can significantly increase matrix modulus [26,27], thereby inhibiting neuronal outgrowth. Elasticity is an important consideration when designing biomaterials for tissue engineering purposes, where matrix stiffness is likely to affect the ability of engrafting neurons or precursors to attach, proliferate, differentiate and ultimately survive.

The objective of this study was to investigate how Young's modulus can influence the formation of neurons from mESC's. In this study, we have taken a novel approach by looking at the effect of Young's modulus on differentiation on a stage-by-stage basis. Previous studies of mechanical effects on differentiation have only been characterised across the entire differentiation process from start to finish, not over individual intermediate stages. The first stage looked at formation of neural precursors from mESC's, the second at immature neurons from neural precursors and the third at more mature types from immature neurons. In order to direct mESC differentiation we used a well characterised adherent monolayer protocol [32,34–36], which avoids the need to create three dimensional aggregates. The material used for the study, GXG, consists of gelatin cross-linked with glutaraldehyde. GXG was chosen as a material as gelatin is also the coating used for Ying et al.'s [32] protocol, allowing for a direct comparison. It has previously been used to characterise mechanical effects on cells in a number of studies [37–39]. Changing the percentage of gelatin in either phosphate buffer saline (PBS) or water varies the Young's modulus of the gel. As tissue from the brain and central nervous system tends to be softer than tissue from other parts of the body, the hypothesis of this study was that softer materials favour the formation of neurons from mESC's over stiffer materials. Cellular attachment, expansion and phenotype changes were investigated for both mESC's and partially -differentiated mESC's at time points of 24 h, 48 h (D2), 72 h, 96 h (D4) and 144 h (D6) in neuronal differentiation medium. Any increase in cell numbers on the materials from 0 h to 24 h was considered as attachment. In addition, any increase in number from 24 h to 72 h was considered expansion. Differentiation was considered from 0 h to 144 h (D6). Finally, inhibitors for myosin-dependent cell contraction and microtubule formation (blebbistatin and nocodazole, respectively) were used in order to elucidate whether either of these cytoplasmic components had an effect on the ability of mESC's and partially-differentiated mESC's to attach to GXG.

2. Materials and methods

2.1. Cell culture

E14Tg2A and 46C mouse embryonic stem cells (Stem Cells Inc., Palo Alto, USA) were cultured on tissue culture flasks (NUNC, Waltham, USA) coated with 0.1% v/v gelatin (Sigma–Aldrich, St Louis, USA) in distilled water. Cells were cultured in the absence of feeder cells and passaged every 2 days. On the day of passaging, cells were washed with phosphate buffer saline (PBS) and trypsinised by incubating with trypsin for 3 min before being resuspended in fresh medium and plated onto fresh gelatin-coated tissue culture polystyrene (TCP) flasks.

MESC's were cultured in GMEM (Invitrogen, Paisley, UK) supplemented with 10% fetal bovine serum (FBS) (Sera Lab, Haywards Heath, UK), 1% Glutamax (Sigma–Aldrich, St Louis, USA), 1% non-essential amino acids (Sigma–Aldrich, St Louis, USA), 1% Antibiotic–Antimycotic (Invitrogen, Paisley, UK), 0.2% β-mercaptoethanol (Sigma–Aldrich, St Louis, USA), and 0.1% LIF (Millipore, Billerica, USA).

For differentiation experiments, cells were harvested by trypsinisation and resuspended in N2B27 medium. N2B27 medium consists of DMEM-F12 (Invitrogen, Paisley, UK) and N2 growth factor (PAA Laboratories, Pasching, Austria) mixed with Neurobasal Medium (Invitrogen, Paisley, UK) and B27 Neuromix growth factor (PAA Laboratories, Pasching, Austria) at a 1:1 ratio.

β-mercaptoethanol (Sigma–Aldrich, St Louis, USA) was added to a final concentration of 0.1 mM from a 0.1 M stock. 1% v/v FBS was added in order to allow mESC's to attach. Cells were then counted and seeded at a density of 1×10^4 cells/cm^2.

For studies using partially-differentiated cells, mESC's were seeded onto TCP in N2B27 medium for 4 or 6 days before being harvested by trypsinisation. Cells were then seeded onto GXG and TCP as with mouse ES cells. 4 days was chosen as the partial-differentiation time as this is the timeframe in which nestin-positive neural precursors begin to substantially appear in colonies when mouse ES cells are differentiated in N2B27 medium (Fig. 2A). 6 days was chosen as a second time-point as this was the when immature neurons begin to form in adherent monoculture [32] (also see Supplementary Fig. 3).

2.2. GXG synthesis

The GXG synthesis protocols were outlined in two earlier studies by Al-Rekabi and Pelling [38,39]. Briefly, stock solutions of gelatin (Sigma–Aldrich, St Louis, USA) were made up in either water or phosphate buffer saline (PBS). Concentrations of gelatin in the solution varied from 3% (corresponding to 2 kPa Young's modulus) in PBS to 4% (18 kPa) and 6% (35 kPa) in water.

The gelatin stock solution was then mixed with glutaraldehyde (Sigma–Aldrich, St Louis, USA) at a ratio of 5 μL glutaraldehyde per 1 mL of gelatin stock solution. The mixture was used to coat 6-well plates and left overnight.

The next day, 1 g/L sodium borohydride (Sigma–Aldrich, St Louis, USA) solution (in PBS) was added to the plates to wash out any residual unreacted glutaraldehyde. After 1 h, plates were washed overnight in PBS. The following day, growth medium (-LIF) was added and plates were allowed to equilibriate for 4–5 h prior to cell seeding.

2.3. Atomic force microscopy

An atomic force microscope (AFM) (Nanowizard I, JPK Instruments, Berlin, Germany) was used to measure GXG Young's modulus. For nanomechancal analysis the AFM was mounted on

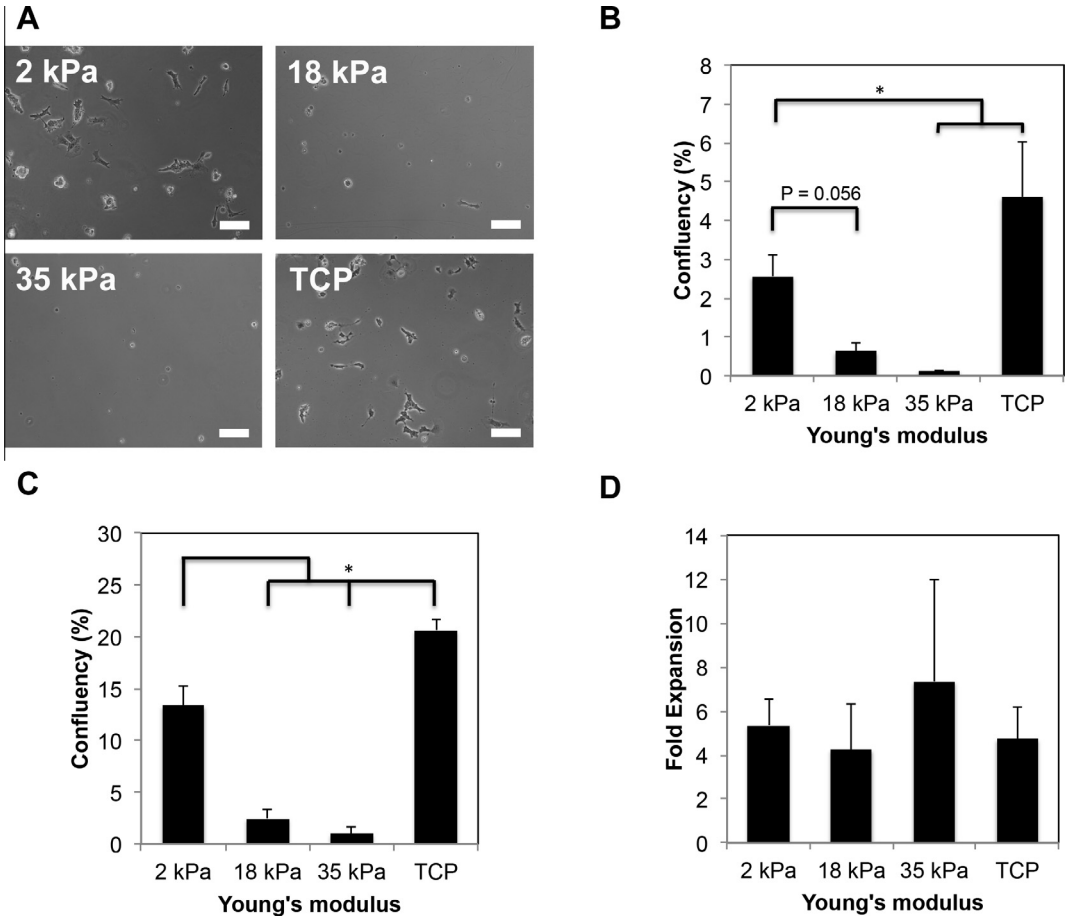

Fig. 1. Attachment of E14 mouse embryonic stem cells in a neurogenic environment is maximised on low modulus substrates. (A) Phase contrast images of mouse embryonic stem cells seeded for 24 h in neurogenic medium upon varying elasticities of GXG and gelatin-coated tissue culture polystyrene (TCP). Scale bars = 100 μm. (B) Analysis of cell confluency from phase contrast images of mouse embryonic stem cells attached for 24 h onto 3 different GXG materials and tissue culture polystyrene. Cell confluency at 24 h decreased with GXG Young's modulus ($p < 0.005$). $^{*}p < 0.05$, as determined by one-way ANOVA analysis followed by Tukey post hoc correction. $N = 3$. (C) Analysis of cell confluency from phase contrast images of mouse embryonic stem cells attached for 72 h onto 3 different GXG materials and tissue culture polystyrene (TCP). Cell confluency at 72 h decreased with GXG Young's modulus ($p < 0.005$). Confluency was again highest on TCP. $^{*}p < 0.005$ as determined by one-way ANOVA analysis, followed by Tukey post hoc correction. $N = 3$. (D) The ratio between confluency at 72 h and 24 h was calculated in order to assess "fold expansion" of colonies post-attachment. No significant difference was found between any of the substrates or across the sample population as a whole. $N = 3$.

an inverted Olympus IX71 (Olympus, London, UK) phase contrast and fluorescence microscope. Force curves were acquired on all gelatine hydrogels with MSCT-AUHW cantilevers (14 ± 5 pN/nm) at 1 Hz and analysed with the Hertz model for a conical indenter [40]. A Poisson ratio of 0.5 was assumed and force curves were analysed for a 200 nm indentation. It should be noted that it is important to characterise the gels before study, as material modulus measurements varied from country-to-country due to, amongst other factors, differences in water ion concentrations (unpublished observation).

2.4. Attachment and expansion study

Undifferentiated or partially-differentiated mouse ES cells were seeded on substrates with varying Young's modulus in N2B27 media. The Young's moduli of the GXG substrates used were 2 kPa, 18 kPa and 35 kPa. TCP was used as a control. The Young's modulus of TCP has been previously measured to be approximately 1 GPa [41] At time-points of 24 h (attachment) and 72 h (expansion), plates were washed with PBS as per a standard adhesion assay in order to remove unadhered cells. Confluency was then calculated from images obtained by phase contrast microscopy. Any cells not in focus in the same plane as the GXG substrate surface during phase contrast microscopy were eliminated from the analyses performed. These cells were observed to be floating in solution above the substrate. The 24-h measurements were used to investigate the effect of Young's modulus on initial attachment of mouse embryonic stem cells in various media, whilst the 72-h measurements showed how Young's modulus affected colony expansion post-attachment.

Images were obtained using a Nikon TE2000-U phase contrast microscope (Nikon Instruments, Kingston, UK) from 5 random fields of view within triplicate wells for each modulus condition. Confluency was then measured using ImageJ software (imagej.nih.gov). Briefly, this involved changing the image setting to a 8-bit monochrome, using the 'fill holes' and 'find edges' functions and varying intensity settings of each image until each cell appeared as a black object on a white background (see Supplementary Fig. 4). The % of each image black compared to white was calculated using the ImageJ software in order to give a value for confluency. Mean confluency for counts were obtained for three wells. A final mean was then taken from triplicate measurements from 3 separate passages. Excel was used in order to calculate standard deviation from the mean.

In order to quantify cell number, a standard curve was created using 20× magnification phase contrast images of mESC's and partially-differentiated cells seeded on GXG and TCP at days 0, 2 and 4. This standard curve was used to calculate the mean cell area.

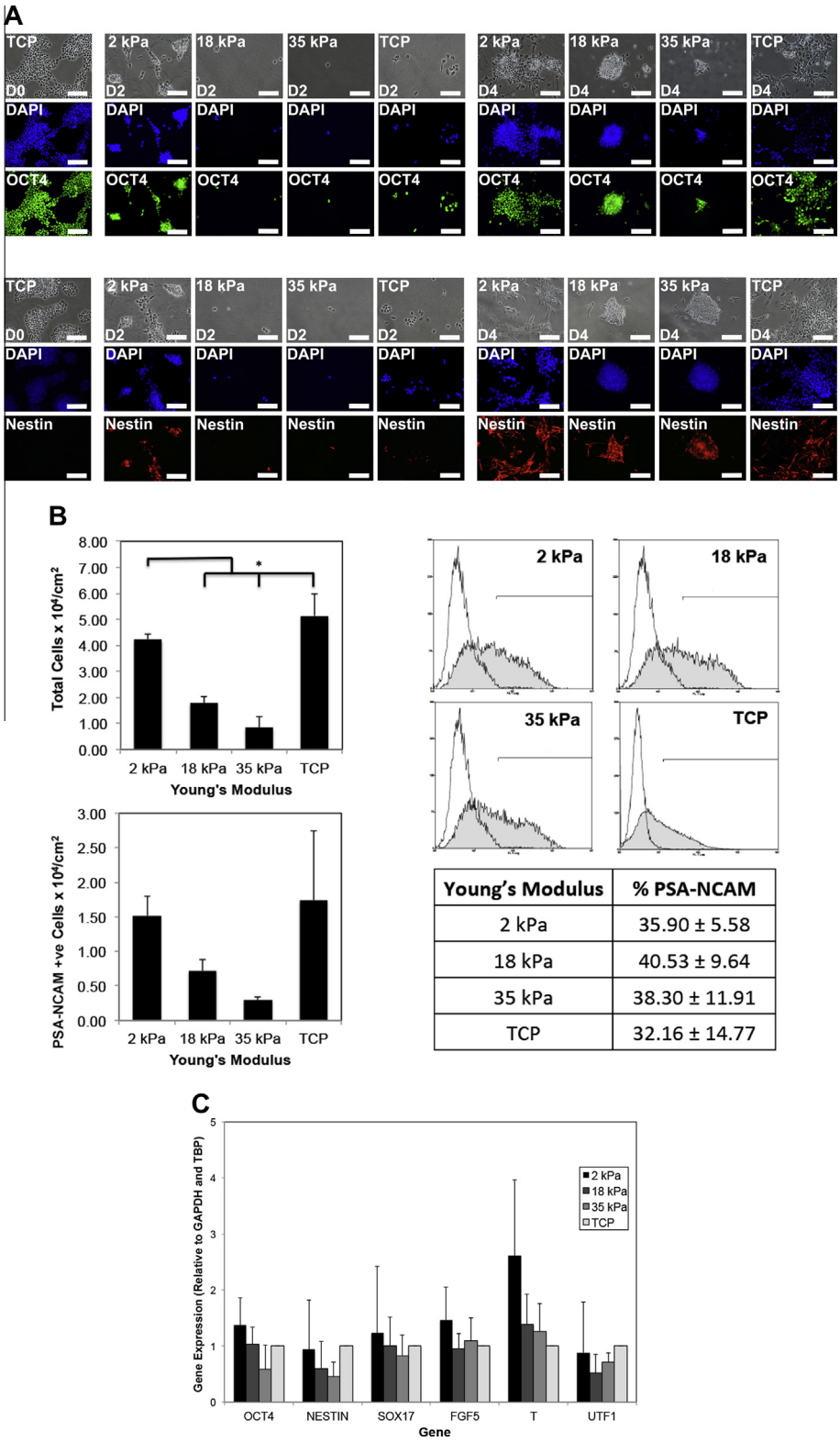

Young's Modulus	% PSA-NCAM
2 kPa	35.90 ± 5.58
18 kPa	40.53 ± 9.64
35 kPa	38.30 ± 11.91
TCP	32.16 ± 14.77

Fig. 2. Neural precursor yield is maximised on soft substrates, but percentage expression of early neural markers does not significantly vary across substrates. (A) Immunostaining for pluripotency marker OCT4 (Green) and neural precursor marker Nestin (Red) at D0 (on tissue culture polystyrene), D2 and D4 (on 2, 18 and 35 kPa GXG as well tissue culture polystyrene) post-seeding. All scale bars = 100 μm. (B) Top-left: total cell concentration ($\times 10^4$ cells/cm^2) at D4 post-seeding is highest upon the softest substrate ($p < 0.005$). Cell counts were obtained using a haemocytometer and divided by the growth surface area to obtain cell concentration values. $^*p < 0.005$ was obtained by one-way ANOVA, followed by Tukey post hoc correction. $N = 3$. Top-right: representative flow cytometry histograms showing expression of PSA-NCAM, a neural precursor adhesion marker. Expression of PSA-NCAM does not significantly vary between substrates. The unshaded distribution represents the isotype control, whilst the shaded distribution represents cells stained with PSA-NCAM. Bottom-right: mean values for PSA-NCAM expression using flow cytometry analysis. Mean % values shown as well as standard deviation from the mean. $N = 3$. Bottom-left: yield of PSA-NCAM positive neural precursors ($\times 10^4$ cells/cm^2). Yield was obtained by multiplying total cell concentration (top-left) by the percentage of cells positive for the marker (bottom-right). $^*p < 0.05$, as determined by one-way ANOVA followed by Tukey post hoc correction. $N = 3$. (C) Relative gene expression of pluripotent (OCT4, UTF1), neural precursor (Nestin) and germ layer (SOX17, FGF5 and T-brachyury) measured using quantitative real-time PCR. $N = 3$. (For interpretation of the references to colour in this figure legend, the reader is referred to the web version of this article.)

The confluency measurements were converted to measurements of total area occupied by cells (the total area of the field of view was calculated using ImageJ). This was divided by the mean cell area to calculated cell enumeration.

2.5. Immunocytochemistry and image analysis

Cells were fixed in 4% v/v paraformaldehyde (Sigma–Aldrich, St Louis, USA) solution for 10 min at 37 °C before being permeabilised for 3 min at 37 °C using 0.1% v/v Triton X-100 (Sigma–Aldrich, St Louis, USA). A blocking solution of 5% v/v FBS was then added for 20 min to prevent non-specific binding.

Cells were then incubated with primary antibodies (1:400 dilution) overnight. The next day, following a wash stage cells were incubated with AlexaFluor (Invitrogen, Paisley, UK) secondary antibodies. Cells were finally incubated with nuclear stains 4′,6-dia midino-2-phenylindole (DAPI, 1:1000 dilution) or Hoescht (1:1000).

Cells were imaged using a Nikon Eclipse TE2000-U phase contrast fluorescence microscope (Nikon Instruments, Kingston, UK).

The percentages of cells positive for MAP2 and βIII tubulin was calculated using image analysis software (imagej.nih.gov). Briefly, the nuclei were first counted to calculate the total cell number. Cells positive for either marker were then counted and compared to the total to give the percentage.

2.6. Flow cytometry

Flow cytometry for polysialic acid neural cell adhesion marker (PSA-NCAM), a cell surface antigen expressed by neural precursor cells [42–45], was performed on cells after 4 days of differentiation on GXG and TCP. Cells were harvested by trypsinisation as before. Counts were then made from the harvested supernatant using a haemocytometer. The cell counts were normalised against the cell surface area to give a calculation of cell concentration.

Cells were then washed in PBS, blocked with 5% FBS before being incubated for 1 h with the PSA-NCAM primary antibody (Millipore, Billerica, USA) at a dilution factor of 1:100. The cells were then further washed before being incubated for 1 h with AlexaFlour 488 secondary antibody (Invitrogen, Paisley, UK). Analysis was performed using a CyAn ADP flow cytometer (Beckman Coulter, Brea, USA). Populations were gated using forward scatter vs side scatter (to isolate viable cells from non-viable cells and debris) and against an isotype control (to eliminate false positives due to non-specific binding).

2.7. qPCR

RNA was first extracted from cell pellets using the RNeasy Micro Kit (Qiagen, Germany) according to the manufacturer's instructions. The RNA was eluted in 12 μL of RNase-free water and the concentration was measured using a Nanodrop spectrophotometer (Thermo Scientific, Delaware, USA), measuring absorbance at wavelengths of 260 nm and 280 nm. 1 mg of RNA was used to synthesise first strand cDNA using the QuantiTect Reverse Transcription kit (Qiagen, Germany), as per the manufacturer's instructions.

For gene expression analysis 1 μL of the cDNA was used in a SYBRGreen real time PCR reaction using the QuantiTect SYBR Green PCR Kit and the pre-validated QuantiTect Primer Assays (Qiagen, Germany) under the manufacturer's protocols, in a CFX Connect Real-Time PCR detection system (Bio-Rad, Hercules, USA). Primer sequences are proprietary but details can be found at https://www1.qiagen.com/GeneGlobe/Default.aspx. Primer assays were as follows: *Oct-3/4* (QT01203748), *Utf1* (QT00252112), *Nestin* (QT00316799), βIII *tubulin* (QT00124733), *Sox17* (QT00160720), *Fgf5* (QT00108906), *T-brachyury* (QT00094430), *TH* (QT00101962) and *GFAP* (QT00101143). For relative quantification, the DDCt method [46] was used. RNA levels were normalised against the housekeeping genes GAPDH and TBP. Expression was quantified as a fold-increase or decrease normalised against TCP. All calculations were performed using the CFX manager software (Bio-Rad, Hercules, USA).

2.8. Blebbistatin and nocodazole inhibition

In order to assess whether basal cell contraction or microtubule stabilisation were necessary for Young's modulus to influence attachment of cells, these two processes were inhibited by small molecule inhibitors blebbistatin [47] and nocodazole [48], respectively. Blebbistatin disrupts cytoskeletal contraction by inhibiting the activity of non-muscle myosin II, a key protein involved in the maintenance of actin cytoskeletal tension [47]. Cells were treated with 50 μM blebbistatin (Sigma–Aldrich, St Louis, USA) for 30 min prior to seeding (as according to the protocol [17]).

For inhibition of microtubule stabilisation, cells were seeded with 10 nM nocodazole (Millipore, Billerica, USA) similarly to the protocol given in [49].

2.9. Statistics

Significant differences within the four-samples (2 kPa, 18 kPa, 35 kPa and TCP) data population were identified using one-way ANOVA analysis, followed by Tukey post hoc correction. The ANOVA analysis identified whether a statistically significant trend occurred across the entire population, whilst the post hoc correction identified where the statistically significant differences lay between individual samples. In the case of the blebbistatin and nocodazole inhibition, where comparisons were made between the untreated and treated condition for each sample, an independent *t*-test was used in order to assess whether differences were statistically significant. All statistical analyses were carried out using the SPSS software (IBM, USA). A confidence interval of 95% (corresponding to a *p*-value less than 0.05) was used in order to designate differences as statistically significant.

3. Results

3.1. GXG substrate characterisation

Three GXG substrates were synthesised by varying gelatin concentration in water or PBS for a given concentration of glutaraldehyde. The stiffness of each substrate was measured using the AFM nanoindentation technique. The substrate stiffness varied from 2 kPa for the softest substrate to 35 kPa for the stiffest material, as detailed in Table 1. Cells were directly adhered to the substrate without requiring additional coating.

Table 1
Relationship between gelatin concentration in PBS or water and GXG Young's modulus.

Concentration (% w/v)	Solution	Young's modulus ± SD
3	Phosphate buffer saline	2.188 kPa ± 0.428
4	Water	18.676 kPa ± 2.373
6	Water	35.167 kPa ± 2.373

The relationship between concentration of gelatin (where percentage related to g/100 mL of solution) and GXG Young's modulus, as measured by atomic force microscopy. GXG was synthesized by mixing the gelatin solution in PBS or water with 5 μL of glutaraldehyde per 1 mL of solution. Modulus was dependent both on concentration and the solution used. Mean value and standard deviation shown. Measurements were obtained from 3 to 5 independent dishes, with 10–25 measurements of Young's modulus per dish.

3.2. Attachment and colony formation of mouse embryonic stem cells (mESC's) on GXG

Mouse embryonic stem cells (mESC's) were seeded onto three different GXG elasticities (2 kPa, 18 kPa and 35 kPa) as well as tissue culture polystyrene (TCP) in N2B27 medium. TCP was used as the 'current best practice' for comparison. However, GXG and TCP are not analogous in their surface chemistry and electro-physical properties. Whilst GXG is already functionalised for attachment (as it based on gelatin, used commonly in normal mESC culture), the TCP is coated with a proprietary surface protein (NUNCLON Delta) for attachment. Furthermore, TCP is functionalised using corona treatment, giving rise to a charged surface for attachment promotion. GXG does not have this property, and is too thick (gels measured approximately 1 mm thick [data not shown]) for the surface chemistry of TCP to affect attachment.

After 24 h, plates were washed with PBS to remove any unattached cells and phase contrast images were obtained (Fig. 1A). As GXG Young's modulus increased, fewer cells appeared to be attached onto the surface of the materials. The cells on the stiffer materials were confirmed as non-apoptotic using an Annexin V assay (Supplementary Fig. 1). Confluency was calculated from the phase contrast images at 24 h post-seeding in order to quantify the levels of cellular attachment (see Section 2 and Supplementary Fig. 2). Cell numbers on each material are shown in Supplementary Fig. 3. As Fig. 1B shows, the highest confluency of cells at 24 h was observed upon the 2 kPa material. There was a 76% decrease in confluence between 2 kPa and 18 kPa ($p = 0.056$) and a 95% decrease between 2 kPa and 35 kPa. Confluence was 80% higher on TCP than on the 2 kPa GXG material. This may have been due to the differences in surface chemistry described above. This effect was conserved ($p < 0.005$ using one-way ANOVA) on a second mESC cell line (Supplementary Fig. 4).

Quantification of GXG cellular confluency at 72 h (Fig. 1C) revealed a similar pattern, with the highest confluence observed on the 2 kPa material, accompanied by a 81% decrease on the 18 kPa and a 93% decrease on the 35 kPa material. Confluency was 54% on the TCP compared to the 2 kPa GXG material.

When confluency at 72 h was divided by the confluency at 24 h (the result being termed 'fold expansion,' representing colony expansion normalised to the initial attachment), it was found that there was no significant variation in expansion between any of the materials ($p = 0.545$ using one-way ANOVA across all four conditions), including TCP. Cells grew as a monolayer and exhibited similar morphology across all materials, and thus we concluded that rate of expansion was similar across the four materials.

The results of the image analysis reveal that attachment of mESC's was highest upon the softest 2 kPa GXG material. This material has a similar Young's modulus to those measured in the early mouse blastocyst (3.39 ± 1.86 kPa [50]), brain [19] and to the mESC's [51] themselves. This was in marked contrast to the stiffer GXG materials, where levels of attachment were far lower. Attachment (but not expansion) on the control was overall higher than on the GXG materials.

3.3. Phenotype and yield of mESC's after 4 days of differentiation on GXG

To investigate the effect of Young's modulus on phenotypic changes during differentiation, immunocytochemistry analysis was performed at day 2 and 4 (post-seeding) of directed differentiation. When stained for the transcriptional factor OCT4 (also known as OCT-3/4), a key marker for pluripotency [52–54], it was found that OCT4 remained expressed until day 4 on all the materials (Fig. 2A). This was an expected result as OCT4 has previously been shown to remain on relatively late during differentiation [55]. Staining for neural precursor [56,57]marker nestin (Fig. 2A), revealed that colonies on all materials contained neural precursors at day 2 and day 4. Nestin was slower to appear in colonies on TCP at day 2, but was abundant in colonies by day 4.

Flow cytometry for neural precursor [42–45] adhesion marker PSA-NCAM was performed at day 4 of mESC neuronal differentiation on the 3 GXG materials and TCP. As shown in Fig. 2B, 30–40% of cells were positive for PSA-NCAM across the materials. There was no significant variation ($p = 0.813$ using one-way ANOVA across all four conditions) in the percentage of PSA-NCAM positive cells at day 4 on any of the three GXG substrates as well as TCP.

Cell counts revealed that the 2 kPa GXG substrate gave rise to the highest cell concentration at day 4, reducing by 57% on the 18 kPa and 80% on the 35 kPa substrate. There was no significant difference in cell count ($p = 0.183$) between the 2 kPa material and TCP. This contrasted with the confluency data comparing the 2 kPa and TCP conditions at 72 h, suggesting that there may be differences in the growth rate during the exponential phase on these two materials. When a time-course fold expansion analysis was performed on the 2 kPa and TCP materials from 2 h post-seeding to 96 h (Supplementary Fig. 5), it was found that beyond 48 h there was a divergence in the expansion profile. This suggests that the 2 kPa has a higher growth rate in the exponential phase than TCP.

The percentage of cells expressing PSA-NCAM was then multiplied by the total cell concentration after 4 days of differentiation in order to calculate the yield of neural precursors from mESC's (Fig. 2B). The yield of PSA-NCAM positive cells was maximised on the soft, 2 kPa GXG material. Yield decreased 54% on the 18 kPa material and 81% on the 35 kPa material (when compared to the 2 kPa material).

Taken together, the data suggests that decreasing Young's modulus increases the yield of neural precursors. The PSA-NCAM flow cytometry data appears to show that this is not due to a direct promotion of neural specification on softer materials. Rather the increased yield on softer GXG materials is due to favourable initial attachment, which leads to the higher cell counts at day 4, as seen in Fig. 2B.

Real-time quantitative PCR (qPCR) was then conducted on cells harvested after 4 days of differentiation upon GXG and TCP to ascertain if Young's modulus had an effect upon gene expression. A total of 7 genes were analysed, including two pluripotency genes (OCT4 [52–54], UTF1 [58]), one neural precursor gene (Nestin [56,57]) and three genes expressed in the each of the three germ layers (Sox17 [59], FGF5 [60], T-Brachyury [61]). The pluripotency and germ layer gene analysis was conducted in order to investigate whether Young's modulus had an impact upon expression of non-neural genes. Expression of non-neural, germ layer genes gives an indication of whether the cells are differentiating homogeneously on the materials, and whether differentiation into non-neural lineages is being promoted by changes in Young's modulus.

It was found that there was no significant variation ($p > 0.05$ in all cases) in gene expression of any of the target genes upon the 3 GXG materials (Fig. 2C). This data suggests that Young's modulus did not affect the expression of key markers associated with the neural differentiation of pluripotent stem cells.

When considered along with the fact that all colonies contain cells positive for nestin, OCT4 (Fig. 2A) and exhibit equal percentages of cells positive for PSA-NCAM (Fig. 2B), these results are further evidence that any increase in yield of neural precursors on soft substrates is due to favourable initial attachment and not a direct promotion of neural specification.

3.4. Effect of blebbistatin and nocodazole on initial attachment of mESC's

Any effect on cellular attachment is likely to be influenced and accompanied by changes to the internal cell structure. The two major structural components of cells are cytoskeletal stress fibres, made up of filaments of F-actin and microtubules, which consist of bundles of α- and β-tubulin. Stress fibres have the ability to contract (with the aid of non-muscle myosin II), allowing for conduction of mechanical signals from the ECM to the nucleus. Mechanosensitive proteins in the nucleus (such as SUN proteins, lamins and nesprins [62]) can then affect a gene expression response based on these mechanical signals. Stress fibres also have the ability to exert forces on the ECM (through focal adhesion complex proteins such as integrins) as well as the ability to increase cell rigidity [61]. Microtubules, which are considerably larger than actin fibres, play a role in determining cell shape [63] and driving the extension of neurites during early neuronal morphogenesis [26].

To elucidate whether the effect of Young's modulus upon cellular attachment was affected by the inhibition of either stress fibre contraction or microtubule stabilisation, cells were treated with small molecule inhibitors for each process. Blebbistatin inhibits the activity of non-muscle myosin II, a protein with a key role in actin stress fibre contraction [64], whilst nocodazole inhibits microtubule formation from tubulin.

When pre-treated with blebbistatin, there was no significant difference ($p > 0.05$ in all cases) in attachment of mESC's at 24 h on any of the 3 GXG substrates or TCP, compared to seeding without blebbistatin (Fig. 3). This implies that any effect of Young's modulus upon attachment of mESC's is independent of myosin-dependent contractions.

When cells were treated with nocodazole, there was no significant difference ($p = 0.322$) in attachment on the 2 kPa GXG material compared to cells that were non-treated. There was however a significant difference ($p < 0.05$) in attachment between the treated and non-treated condition on the 18 kPa material, where confluency decreased by 71%. There was a difference between treated and non-treated on the 35 kPa material, where confluence decreased by 44%. However, this was statistically non-significant ($p = 0.056$). There was no difference in attachment between the treated and non-treated condition on TCP. It is possible that attachment may be dependent on microtubule stabilisation particularly on stiffer GXG materials however further experimentation is needed before this can be confirmed. There is also evidence that nocodazole treatment can result in an increase in stress fibre organisation [65,66]. This would imply that stress fibre organisation is detrimental to attachment of mESC's on stiff materials, which would be counter-intuitive when compared to other cell types such as fibroblasts [23].

3.5. Attachment and colony formation of four-day partially-differentiated mESC's on GXG

Similar experiments to above were conducted with partially-differentiated cells in order to assess whether these effects change as cells become more mature. Mouse ESC's were first partially-differentiated in N2B27 medium for 4 days on TCP, before being trypsinised, resuspended in fresh N2B27 medium and seeded onto the GXG materials and TCP. When mESC's were partially-differentiated for four days in N2B27 medium, large colonies of neural precursors formed. Most cells within these colonies were positive for nestin and OCT4 (Fig. 2A). Furthermore, 32% of cells at day four of differentiation were positive for PSA-NCAM (Fig. 2B). Confluency measurements were made from 24 h and 72 h phase contrast images in a similar manner as for the undifferentiated cells. Cell numbers are shown in Supplementary Fig. 6.

As Fig. 4A and B show, the 2 kPa GXG substrate gave rise to the highest confluency after 24 h. Confluency on the hardest substrate (35 kPa) was 83% lower than the softest substrate (2 kPa), indicating a stark decrease in attachment with increasing stiffness. This implies that the partially-differentiated cells retain the mechanical sensitivity of undifferentiated cells to attachment. Interestingly, attachment on the 2 kPa was high compared to that of the TCP, where confluency decreased 69% compared to the soft material. This was in contrast to our findings with the undifferentiated cells. This may be due to mESC's being adapted for long-term growth on non-physiological TCP. Once they begin to differentiate and form developed cytoskeletal structures, they appear to lose this adaptation and gain a preference for attachment on the most physiologically relevant material. A recent study has shown that mesenchymal stem cells retain mechanical information from

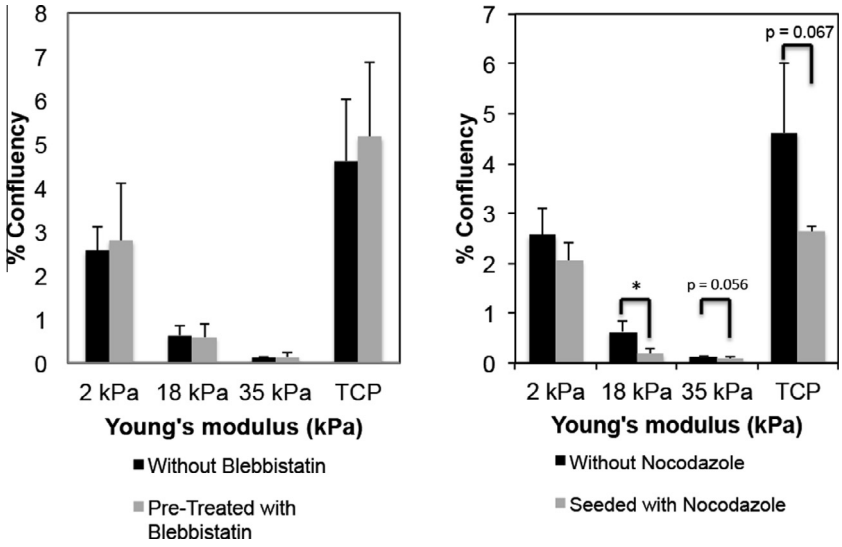

Fig. 3. Preferable attachment of mouse embryonic stem cells on stiffer substrates is dependent on microtubule stabilisation, but not myosin-dependent basal cell contraction. (A) Comparison of cell confluency at 24 h on GXG and tissue culture polystyrene with and without pre-treatment with blebbistatin. No significant difference was found using independent samples *t*-test at 24 h when cells were seeded with the inhibitor compared to without. $N = 3$. (B) Comparison of cell confluency at 24 h of GXG and tissue culture polystyrene with and without addition of nocodazole. $^{*}p < 0.05$ as determined by independent samples *t*-test. $N = 3$.

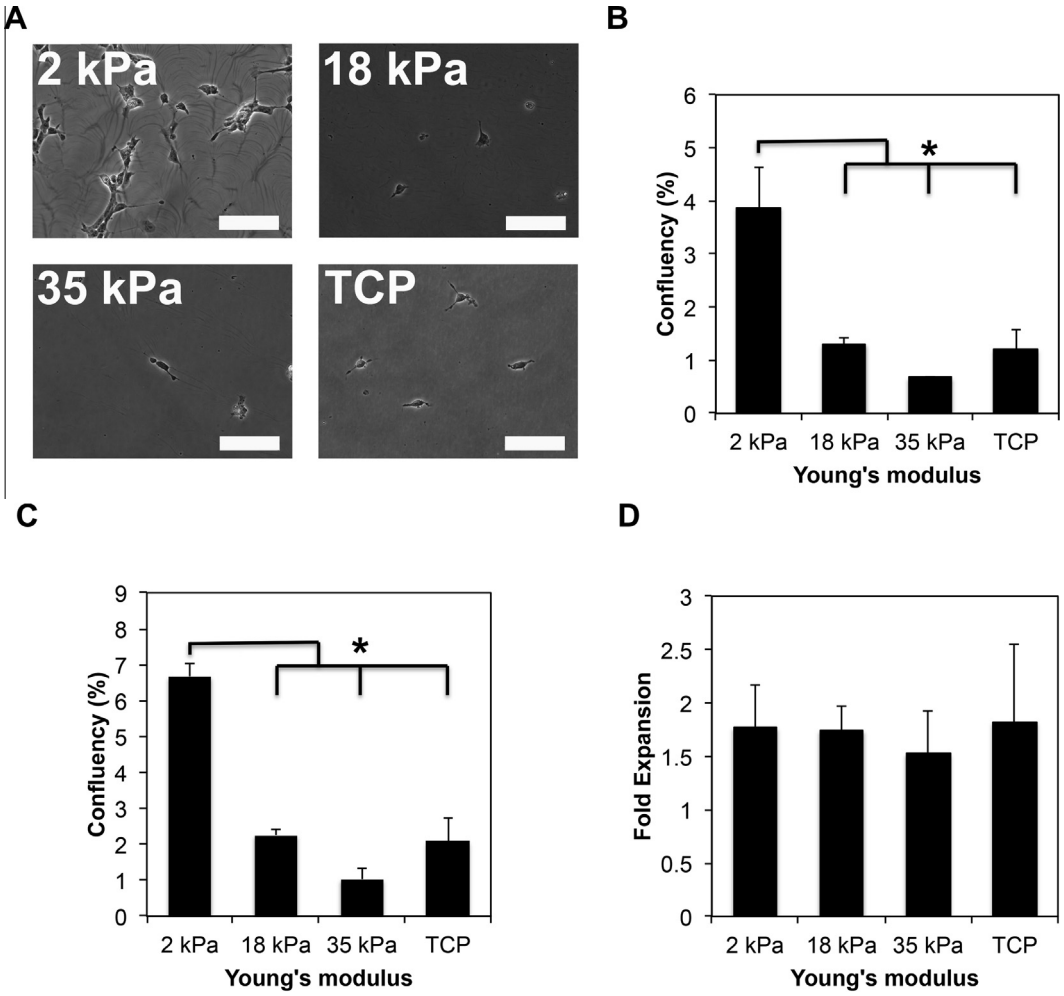

Fig. 4. Attachment of neural precursors is maximised on low modulus substrates. (A) Phase contrast images of four-day partially-differentiated cells (mESC's differentiated for four days in N2B27 on TCP) seeded for 24 h upon varying elasticities of GXG. Numbers of attached cells observed decreases as GXG Young's modulus increases. Gelatin-coated TCP is shown as a control, representing current best practice in the laboratory. Scale bars = 100 μm. (B) Analysis of cell confluency from phase contrast images of four-day partially-differentiated cells attached for 24 h onto 3 different GXG materials and TCP. Confluency at 24 h decreased with Young's modulus ($p < 0.005$). $^{*}p < 0.005$, as determined by one-way ANOVA followed by Tukey post hoc correction. $N = 3$. (C) Analysis of cell confluency from phase contrast images of four-day partially-differentiated cells attached for 72 h onto 3 different GXG materials and tissue culture polystyrene. Confluency decreased with Young's modulus ($p < 0.005$). $^{*}p < 0.005$, as determined by ANOVA analysis followed by Tukey post hoc correction. $N = 3$. (D) The ratio between confluency at 72 h and 24 h was calculated in order to assess "fold expansion" of colonies post-attachment. No significant difference was found between any of the substrates or across the sample population as a whole, when one-way ANOVA was carried out, followed by Tukey post hoc correction. $N = 3$.

culture on tissue culture plastic when transferred onto soft materials [67].

The same pattern was conserved at 72 h, where confluency was highest on 2 kPa. Confluency was 66% lower on 18 kPa and 84% lower on 35 kPa. Again confluency was significantly ($p < 0.005$) higher on the softest material when compared with TCP controls. When 72 h confluency was compared to 24 h confluency, fold expansion between these times did not vary significantly ($p = 0.874$ using one-way ANOVA across all 4 samples) on any of the materials. This implies that whilst Young's modulus affects the attachment of partially-differentiated cells, it did not have a direct effect upon their subsequent expansion. This was consistent with our findings with undifferentiated cells.

3.6. Phenotype and yield of four-day partially-differentiated mESC's after 4 days of differentiation on GXG

Cells partially-differentiated for 4 days on TCP were harvested and seeded onto GXG and TCP for a further 4 days in N2B27 medium. Immunocytochemistry analysis was then conducted on cells for β-III tubulin, a marker for neurite formation used to identify the earliest neurons formed during stem cell neuronal differentiation [68–70]. Staining (Fig. 5A) revealed that characteristic β-III tubulin positive cells with neurite extensions formed in colonies on all materials.

For yield and flow cytometry analysis, mESC's were partially-differentiated for 4 days on TCP, before being seeded onto GXG and TCP. They were then differentiated for a further four days on GXG and TCP in N2B27 medium before being harvested for cell concentration and flow cytometry analysis. Total cell concentration dramatically decreased with increasing stiffness (Fig. 5B), reducing by 80% on the hardest substrate (35 kPa) compared to the softest (2 kPa). This was consistent with the earlier results with mESC's. However, as with the attachment data, the cell concentration on TCP decreased (by almost 60%) when compared to 2 kPa. This again implies that there is a loss of adaptation to tissue culture polystyrene growth occurring with differentiation.

Flow cytometry analysis revealed that there was no significant variation ($p = 0.583$) in the percentage of cells positive for PSA-NCAM marker (between 60% and 75% of cells were positive)

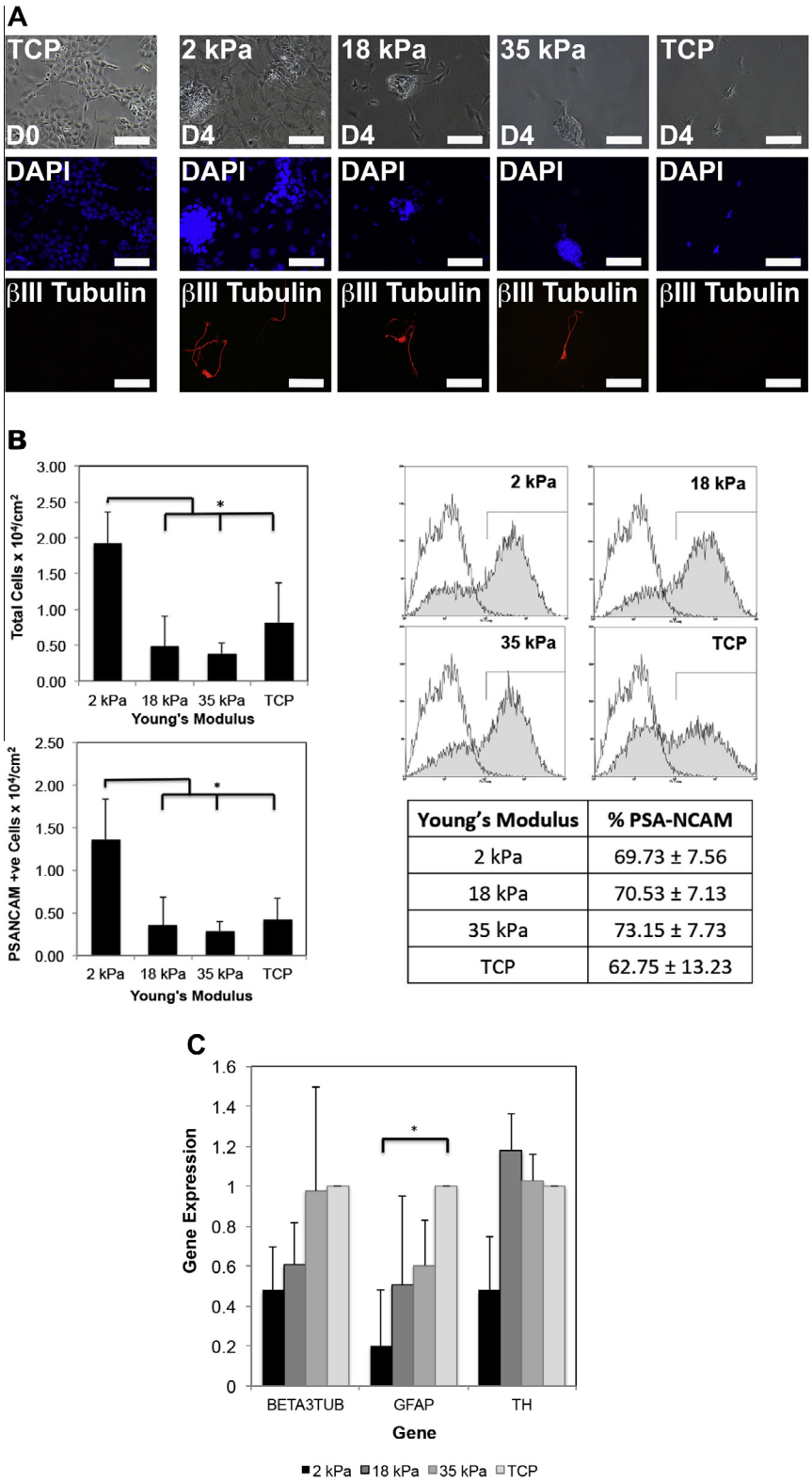

Fig. 5. Neural precursor yield is maximised on soft substrates, but percentage expression of mid/late neural markers does not significantly vary across substrates. (A) Immunocytochemistry analysis for neuronal marker β-III tubulin (Red) at D0 (on tissue culture polystyrene) and D4 on 2, 18 and 35 kPa GXG as well tissue culture polystyrene post-seeding. All scale bars = 100 μm. (B) Top-left: total cell concentration ($\times 10^4$ cells/cm^2) at D4 post-seeding was highest upon the softest substrate ($p < 0.01$). Cell counts were obtained using a haemocytometer and divided by the growth surface area to obtain cell concentration values. $^*p < 0.05$, as determined by one-way ANOVA followed by Tukey post hoc correction. $N = 3$. Top-right: representative flow cytometry histograms showing expression of PSA-NCAM. Expression of PSA-NCAM does not significantly vary between GXG substrates. The unshaded distribution represents the isotype control, whilst the shaded distribution represents cells stained with PSA-NCAM. Bottom-right: mean values for PSA-NCAM expression using flow cytometry analysis. Mean % values shown as well as standard deviation from the mean. $N = 3$. Bottom-left: yield of PSA-NCAM positive neural precursors ($\times 10^4$ cells/cm^2). Yield was obtained by multiplying total cell concentration (top-left) by the percentage of cells positive for the marker (top-right). $^*p < 0.05$ was determined by one-way ANOVA followed by Tukey post hoc correction. $N = 3$. (C) Relative expression of neuronal (β-III tubulin, TH) and astrocyte (GFAP) genes measured using quantitative real-time PCR. $^*p < 0.05$ was determined by one-way ANOVA followed by Tukey post hoc correction. $N = 3$. (For interpretation of the references to colour in this figure legend, the reader is referred to the web version of this article.)

between the 3 GXG substrates and TCP (Fig. 5B). The percentage range markedly contrasts with the earlier data in Fig. 2B, where 30–40% of cells were shown to express PSA-NCAM. This illustrates that the cells used in the partial-differentiation experiments were more mature than the cells used in Figs. 1–3 and that cells continued to differentiate following the replating process.

We next calculated the total yield of neural precursor cells by multiplying the total cell concentration by the percentage of cells expressing PSA-NCAM. Yield (Fig. 5B) was significantly higher on the 2 kPa material when compared to the harder substrates, exemplified by a 80% rise when compared with 35 kPa. Unlike earlier experiments with undifferentiated mESC's, the softest substrate (2 kPa) also performed better than traditional TCP resulting in a 69% rise in the number of neural precursors. However, as with the mESC's, this increase in yield is due to favourable initial attachment rather than direct promotion of neuronal differentiation.

Gene expression of neuronal genes β-III tubulin and TH (tyrosine hydroxylase, for dopaminergic neurons [71]) following four days of differentiation of partially-differentiated cells did not vary significantly with Young's modulus (Fig. 5C). This was similar to our findings using undifferentiated cells. However, in this case expression of GFAP (glial fibrillary acidic protein), a gene used as a marker for astrocytes [72] decreased 80% ($p < 0.05$) on the 2 kPa GXG material compared to TCP. This implies that gene expression becomes sensitive to Young's modulus as cells mature away from the undifferentiated state, and that the initial sensitivity in gene expression is restricted to astrocyte-specific genes rather than neuronal.

3.7. Effect of blebbistatin and nocodazole on the initial attachment of four-day partially-differentiated mESC's

To investigate whether the disruption of myosin-dependent contraction or microtubule stabilisation would have an effect upon initial attachment of partially-differentiated cells, cells were treated with blebbistatin or nocodazole, respectively. When pre-treated with blebbistatin, it was found that the number of cells attaching to all 3 GXG substrates halved when compared to untreated cells (Fig. 6). These results imply that, unlike undifferentiated cells (Fig. 3), the attachment of partially-differentiated cells upon all materials is dependent on basal cell contraction, mediated by myosin. Undifferentiated mESC's can adhere to materials with minimal cytoskeletal organisation [73,74] whilst more mature cells tend require substantial amounts of actin stress fibre formation in order to adhere to the extracellular matrix. Cytoplasmic F-actin in these cells on the varying GXG materials was visualised by immunocytochemistry in Supplementary Fig. 7.

Conversely, there was no difference in the initial attachment of partially-differentiated cells for any of the 3 GXG materials as well as TCP when seeded with nocodazole, an inhibitor of microtubule stabilisation compared to the untreated condition.

This was in contrast with the findings with undifferentiated cells (Fig. 3), where attachment decreased on the 18 kPa, 35 kPa and TCP materials. This implies that, unlike basal contraction, microtubule formation was not a prerequisite for partially-differentiated cell attachment onto materials of any elasticity, which is consistent with findings for other differentiated cell types. Microtubule formation in neurons is usually associated with cellular elongation and branching rather than attachment [75,76].

3.8. Attachment and expansion of six-day partially-differentiated neurons

For the final experiments, mESC's were allowed to partially-differentiate further in N2B27, for six days on TCP prior to seeding onto GXG and TCP. At this stage, immature neurons begin to form in colonies (Supplementary Fig. 8). The aim of these experiments was to look at the effect of Young's modulus on attachment and expansion at a later stage of differentiation, when β-III tubulin-positive neurons (the earliest to form during stem cell neuronal differentiation) mature into post-mitotic, functional MAP2-positive neurons. Confluency was measured at 24 h and 72 h once again to assess whether Young's modulus affected attachment and expansion of these immature neurons.

Unlike the previous cell types (mESC's and four-day partially-differentiated cells), attachment of six-day partially-differentiated cells at 24 h did not significantly ($p = 0.481$) vary between any of the four materials (Fig. 7A and B), including TCP. This result suggests that the effect of Young's modulus on attachment during mESC neuronal differentiation is dependent upon the maturity of the starting cell population. The effect on attachment diminishes as cells become more mature.

As at 24 h, confluency at 72 h did not vary significantly ($p = 0.541$) between any of the four materials. When 72 h

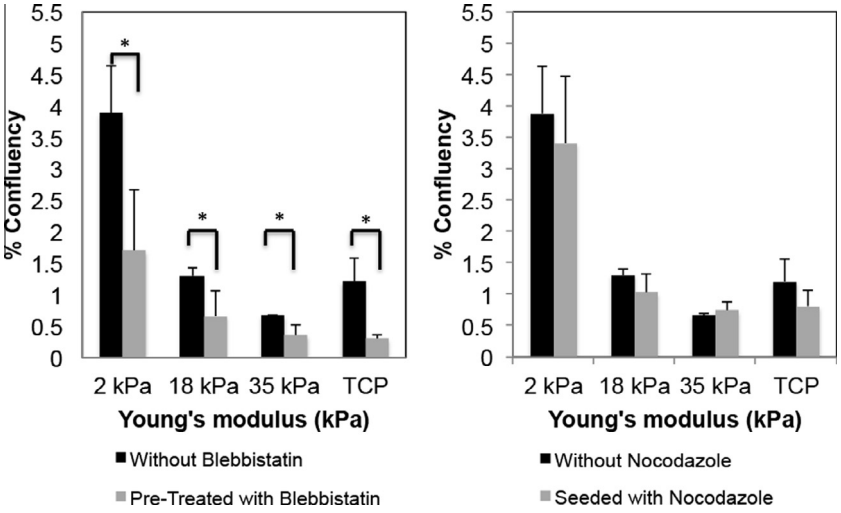

Fig. 6. Attachment of pre-differentiated cells on all substrates is dependent on myosin-dependent basal contraction, but not on tubulin stabilisation. (A) Comparison of cell confluency at 24 h on GXG and TCP with and without pre-treatment with blebbistatin. $^{*}p < 0.05$, as determined by independent samples *t*-test. $N = 3$. (B) Comparison of cell confluency at 24 h on GXG and tissue culture polystyrene with and without the addition of nocodazole. There was no significant decrease in attachment on any of the 4 materials, as determined by independent samples *t*-test. $N = 3$.

confluency was compared to 24 h, the resulting fold expansion did not vary significantly ($p = 0.808$) between the four materials. In conclusion, Young's modulus had no effect upon expansion of six-day partially-differentiated neurons. This was consistent with both previous cell types (mESC's and four-day partially-differentiated cells) and suggests that the effect of Young's modulus on expansion is unaffected by starting population maturity, unlike attachment.

3.9. Phenotype of six-day partially-differentiated neurons after 6 days of differentiation on GXG

Mouse ESC's partially-differentiated for six days in N2B27 medium on TCP were trypsinised, resuspended and seeded onto GXG and TCP for a further six days in N2B27. Day six is where β-III tubulin begins to appear in monolayer differentiation (Supplementary Fig. 4). Immunocytochemistry was then performed for two markers; β-III tubulin and MAP2, a marker for mature neurons [77–79] (not observed at day six of mESC monolayer neuronal differentiation). Staining for β-III tubulin revealed extensive neurite formation on the 2 kPa and 18 kPa materials (Fig. 8A). 13.60% and 14.36% of cells were positive for β-III tubulin on the 2 kPa and 18 kPa GXG substrates respectively (Table 2). Formation of β-III tubulin positive neurites was still extensive across the culture surface on the stiffer 35 kPa material, albeit not as abundantly as the softer GXG materials (3.40% were positive as seen in Table 2). This implies that for cells in the later stages of neuronal differentiation, the effect of Young's modulus on the survival of neuronal phenotypes becomes attachment-independent. There were no neurites on the TCP material (Table 2). This also contrasts with the results found for the earlier stages of differentiation. Although mESC's are adapted for growth on gelatin-coated tissue culture polystyrene, it may be that this adaptation is lost as they undergo phenotype changes during differentiation.

Staining for MAP2 revealed that the most mature neuron formation was found on the softest, 2 kPa material (Fig. 8B). 5.15% of cells were positive for MAP2 on this material (Table 2). Mature neuron formation was negligible on the intermediate 18 kPa material (0.95% were positive as seen in Table 2), despite overall confluency and cell density being similar. No mature neurons formed on the stiffest 35 kPa and TCP materials (Table 2). This suggests that soft materials favour the formation of mature neurons from immature neurons compared to stiffer materials, in contrast to the findings using mESC's (Fig. 2) and four-day partially-differentiated cells

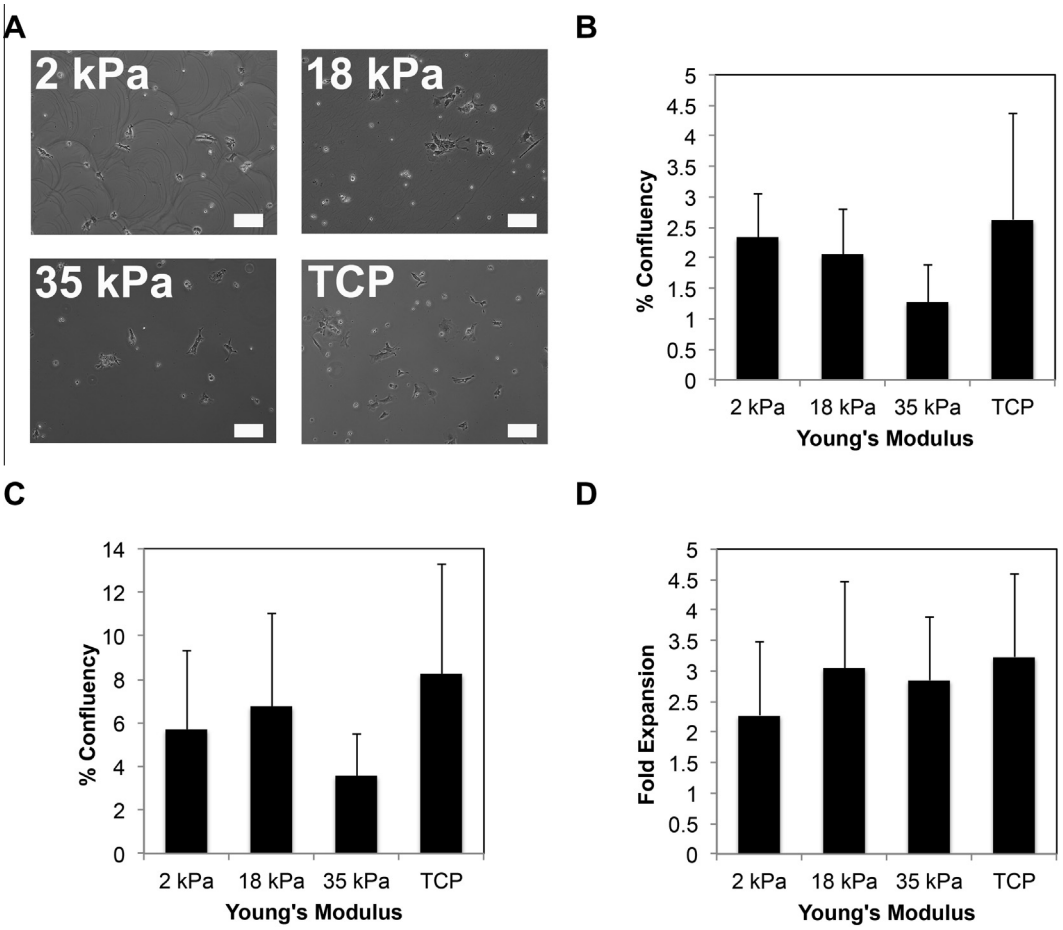

Fig. 7. Attachment of immature neurons is unaffected by Young's modulus. (A) Phase contrast images of six-day partially-differentiated neurons (mESC's differentiated for six days in N2B27 on TCP) seeded for 24 h upon varying elasticities of GXG. Gelatin-coated TCP is shown as a control, representing current best practice in the laboratory. Scale bars = 100 μm. (B) Analysis of cell confluency from phase contrast images of six-day partially-differentiated neurons attached for 24 h onto 3 different GXG materials and TCP. No significant difference was found between any of the substrates or across the sample population as a whole, when one-way ANOVA was carried out, followed by Tukey post hoc correction. $N = 3$. (C) Analysis of cell confluency from phase contrast images of six-day partially-differentiated neurons attached for 72 h onto 3 different GXG materials and tissue culture polystyrene. No significant difference was found between any of the substrates or across the sample population as a whole, when one-way ANOVA was carried out, followed by Tukey post hoc correction. $N = 3$. (D) The ratio between confluency at 72 h and 24 h was calculated in order to assess "fold expansion" of colonies post-attachment. No significant difference was found between any of the substrates or across the sample population as a whole, when one-way ANOVA was carried out, followed by Tukey post hoc correction. $N = 3$.

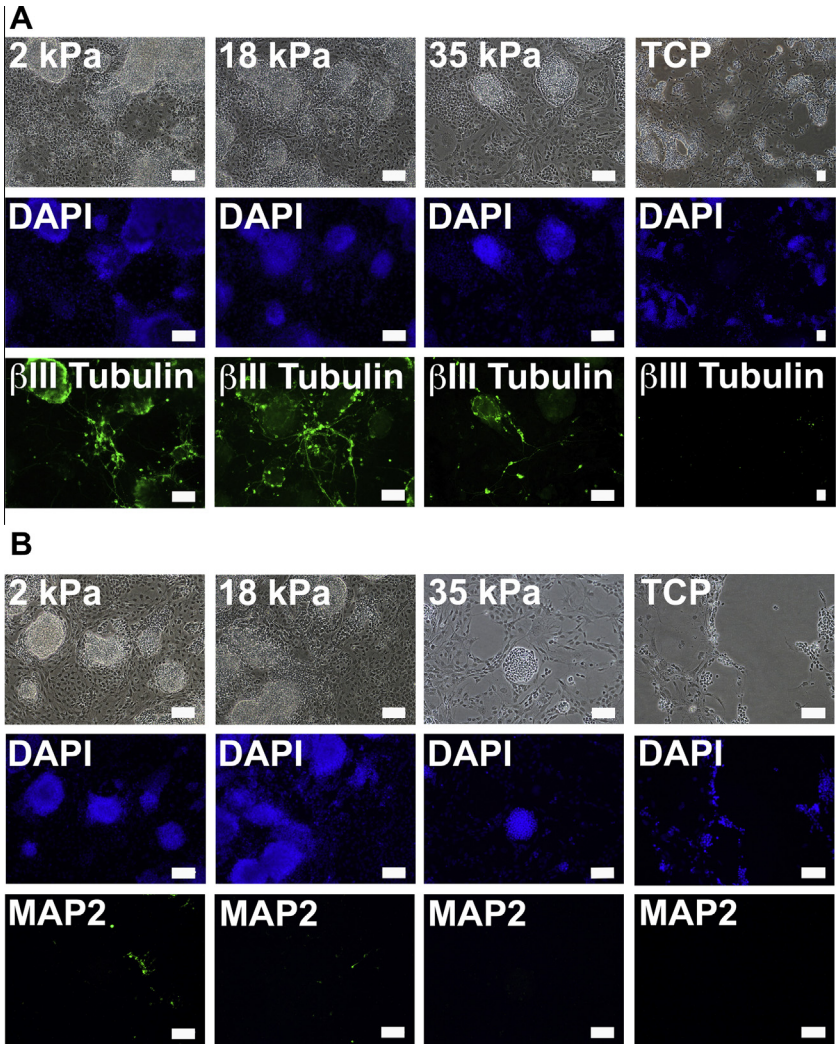

Fig. 8. Formation of MAP2-positive neurons from pre-differentiated neurons is maximised on soft materials. (A) Immunocytochemistry analysis for β-III tubulin at D6 on 2, 18 and 35 kPa GXG materials. TCP was used as a control. All scale bars = 100 μm. β-III tubulin-positive neuron formation was maximised on the 2 kPa and 18 kPa materials over 35 kPa and TCP (formation of neurons was negligible on the latter). (B) Immunocytochemistry analysis for MAP2, a marker for mature neurons at D6 on 2, 18 and 35 kPa GXG materials. TCP was used as a control. All scale bars = 100 μm. MAP2-positive mature neuron formation was maximised on the 2 kPa materials over the 18 kPa, 35 kPa and TCP materials (formation was negligible on the latter two materials).

Table 2
Quantification of cells positive for MAP2 and βIII tubulin on varying Young's moduli on day six of differentiation.

	2 kPa	18 kPa	35 kPa	TCP
% +ve for βIII tubulin	13.60%	14.36%	3.40%	0%
% +ve for MAP2	5.15%	0.95%	0%	0%

Cells were partially differentiated for 6 days on TCP before being seeded onto 2, 18, 35 kPa GXG materials and TCP for 6 days in differentiation medium. % of cells positive for MAP2 and βIII tubulin was quantified using image analysis. The total number of cells was counted using DAPI, a nuclear stain. The number of cells positive for each marker was divided by this figure to give a % value.

(Fig. 5). Thus, the effect of Young's modulus on the changes in phenotype during differentiation are dependent upon the maturity of the starting population.

4. Discussion

The attachment of both mESC's and four-day partially-differentiated cells in N2B27 neural differentiation medium was optimum on soft materials. The stiffness of the substrate is thus clearly an influential cue for cell recruitment during early neuronal differentiation. Small molecule inhibition of basal cell contraction decreased attachment on all materials for partially-differentiated cells, but had no effect on mESC's. Unlike mESC's [73], neural cells polymerise actin into organised, stress fibres [26]. The decrease in attachment occurs across all materials, which is logical as neuronal cells have previously been shown to polymerise actin equally on soft and stiff materials [26]. This suggests that there is another mechanistic pathway responsible for the variations in attachment on different materials.

TCP exhibited increased attachment when compared to the stiffer materials. Although TCP has a significantly higher Young's modulus than the range studied here, we would not expect a GXG-type material with a TCP-like Young's modulus to behave similarly to TCP. TCP is fundamentally different as a substance to GXG, in both biochemical and electrochemical terms, as described earlier. We have chosen to describe changes within the GXG Young's moduli under study and any transitions described are for this range only.

A further possible explanation for this effect may be some retention of some mechanical memory from expansion on TCP prior to differentiation, influencing their ability to grow on softer materials compared to TCP. This has previously shown to occur in mesenchymal stem cells [67]. Future studies could look at

whether expansion on soft gels prior to seeding would affect the mESC's fate decisions. Culturing cells in expansion medium on soft gels showed the same pattern as in differentiation medium (Supplementary Fig. 9). Similarly, partially differentiating cells on varying gel elasticities for six days before replating on equivalent elasticities had no overall effect on growth compared to partially differentiating on TCP (Supplementary Fig. 10).

When mESC's were partially-differentiated for six days, Young's modulus did not have an effect upon attachment. This suggests that a rapid change in mechanosensitivity occurs as cells mature from being β-III tubulin negative at day four of partial-differentiation (where attachment is sensitive to Young's modulus) to being β-III tubulin positive at day six of partial-differentiation (Supplementary Fig. 3). The effect of Young's modulus on attachment is therefore dependent on the maturity of the starting population. In previous investigations, attachment of neural precursors [26–28] have also been observed to be independent of Young's modulus.

The mechanism behind the effect of stiffness on attachment is likely to involve interactions between the ECM, proteins found in the soluble microenvironment and, crucially, integrin proteins on the cell surface. One particular protein, vitronectin (a component of fetal bovine serum) strongly promotes mESC attachment [80] by adsorbing onto tissue culture surfaces [81]. In the case of mESC's and four-day partially-differentiated cells, one possibility is that soft substrates are preferentially adsorbing vitronectin onto their surfaces in order to increase interactions with $\alpha v\beta_1$, $\alpha v\beta_3$ and $\alpha v\beta_5$ [82] integrins on the cell surface. More interactions between the ECM and integrins may have led to the high levels of cell attachment seen on softer substrates. Adhesion of neuronal cells such as the six-day partially-differentiated cells is not strongly influenced by serum vitronectin [83,84] (they attach in serum-free medium), which may explain why their attachment is unaffected by stiffness.

Expansion of colonies beyond the initial attachment did not vary between materials for any of the cells studied. The influence of Young's modulus on expansion is thus independent of cellular maturity. Other studies to date, in mESC's [85], human ES cells [21,86] and neural stem cells [30] have also demonstrated that expansion and proliferation do not vary with modulus. In a study using primary neuronal precursors [28], proliferation was found to increase with Young's modulus. Unlike our experiments this was in medium developed to expand neuronal precursors rather than promote differentiation of undifferentiated cells. Proliferation of both mESC's and neural stem cells is strongly regulated by the mammalian target of rapamycin (mTOR) signalling pathway [87,88]. One possibility is that stiffness is unlikely to modulate this pathway as it is regulated by E-cadherin [89], a cell surface protein that links cells to other cells rather than to the ECM (as integrins do).

In the main part Young's modulus did not have an effect on the phenotype of cells formed following differentiation for mESC's or four-day partially-differentiated cells. Any increase in yield of neuronal cells on the softest substrate (Figs. 2B and 5B) was due to an increase in the percentage of cells in the initial inoculum that were able to attach at the beginning of differentiation (Figs. 1 and 4), rather than a direct neurogenic effect of the material. In one case, soft materials reduced expression of GFAP, an astrocytic gene, in four-day partially-differentiated cells (Fig. 5C). For six-day partially-differentiated cells, the softest material increased the number of MAP2-positive neurons (Fig. 8B) following differentiation, without affecting initial attachment. This implies that soft materials directly promote maturation of six-day partially-differentiated cells, in contrast to our findings using less mature cells.

Previous work measuring changes in ES cell gene expression have shown a variety of effects. In both mouse [85] and human [21] ES systems it has been shown, in accordance to our findings that there is no variation in ectoderm gene expression with modulus (in undirected differentiation medium). This implies that gene expression is less sensitive to Young's modulus in undifferentiated ES cells than more mature cells. When neuronal differentiation was directed in mouse EB's plated onto 2D substrates, the percentage of cells positive for neuronal markers increased with Young's modulus [90], (albeit from 10 Pa to 1 kPa, a low modulus range compared to our study). This implies that the 1 kPa modulus order of magnitude represents a peak, with differentiation efficiency reducing either side. Three-dimensional EB's are not directly analogous to monolayers of mESC's, however as only a fraction of the cells are directly in contact with the substrate. Both Banerjee et al. and Saha et al.'s studies [29,30] showed that there was no difference in β-III tubulin expression in differentiating neural stem cells when modulus was increased. Georges et al., contradictorily showed an increase in percentage of mixed cortical neurons positive for β-III tubulin with a decrease in modulus [26]. As mixed cortical neurons are more mature than neural stem cells, this reinforces our claim that the impact of Young's modulus on phenotype changes is a maturity dependent effect. It also implies that four-day partially-differentiated cells are closer to neural stem cells in phenotype, whilst six-day cells are closer to more mature, neuronal precursors. In both mixed cortical neurons [26] and neural stem cells [30], astrocytes tended to grow more favourably on stiffer materials, in agreement with our study. Previous studies using human pluripotent stem cells have also shown soft materials to favour formation of MAP2-positive neurons, dependent on YAP coactivation [91]. An earlier study [28] demonstrated that the number of primary mixed hippocampal cells positive for MAP2 did not vary with modulus from 1 kPa to 7 kPa. A second study by the same group [92] produced the same result in mixed spinal cord neural precursors. When these spinal cord neural precursor cells were then purified however, the percentage of cells positive for nestin (at D2) and MAP2 (at D5) decreased with an increase in Young's modulus (6 kPa to 27 kPa). The presence of mature, non-neural cells may interfere with the stiffness effects, as these cells may be promoting maturation through their own cytokine or cadherin-based cell–cell signaling.

Our findings suggest that the effect of Young's modulus on neuronal specification varies as the identities of the starting cells change. As mESC's differentiate, their cytoskeletons develop a more organised structure. Cells with organised, pre-stressed actin fibres are able to sense the mechanical deformation of the extracellular matrix and direct gene expression accordingly [62]. This occurs through communication between the actin cytoskeleton and mechanosensitive LINC complex proteins (nesprins, SUN and lamins) in the cell nucleus [62]. Mouse ES cell gene expression appears to be mechanically insensitive. Four-day partially-differentiated cells develop more cytoskeletal structure. At this stage, the fate decision between the astrocytic and neuronal lineage becomes sensitive to Young's modulus, implying that there is some 'hard-wiring' of astrocyte genes to the cytoskeleton. At the six-day partially-differentiated stage, it is the neuronal genes that appear to be hard-wired to the cytoskeleton. The result in this hard wiring change is that less mature cells are sensing their mechanical microenvironment in order to decide to commit between the neuronal and glial fate, whilst the more mature cells appear to be choosing between various neuronal fates.

These findings have a number of potential implications in terms of cell therapy bioprocessing. The choice of biomaterial modulus for differentiation will influence how well ES cells attach and neural precursors mature. In addition to this, GXG is a suitable material for tissue engineering, owing to its biocompatibility, biodegradability and stability in long term culture [93]. The low raw material cost, ease of availability and ease of synthesis of

GXG over other biomaterials can also potentially reduce process costs and labour requirements. Further investigation into other differentiation systems may provide similarly interesting findings. However, this may require testing of moduli outside of the range tested within this study.

The results may also give some hints as to how cells may behave when introduced into the diseased environment. Spinal cord injury sites are commonly characterised by abnormal tissue stiffness, which may be caused by scarring, fibrosis and glial hypertrophy [26,49]. If less differentiated cells are introduced into these areas, it is likely they will be unable to attach. Glial hypertrophy in lesion areas also often result in cells being unable to respond to supportive growth factors [94], possibly reducing any cooperative effects between the soluble and mechanical microenvironments. Investigating effects of Young's modulus stage-by-stage *in vitro* may also provide some clues as to how cellular responses to Young's modulus vary during gastrulation and early development.

5. Conclusions

Soft materials, with Young's modulus similar to that of mouse blastocysts, the developing brain and spinal cord, increase the yield of neurons from mESC's. In mESC's and four-day partially-differentiated cells, this increase is due to increased initial attachment of cells and not direct promotion of the neuronal fate. In mESC's, attachment on the stiffest materials is dependent upon microtubule stabilisation whilst in neural stem cells attachment on all materials is dependent upon myosin-dependent contraction. The influence of Young's modulus on attachment decreases as cells become more mature (having no effect on six-day partially-differentiated cells). Conversely, the influence of Young's modulus on phenotype changes during differentiation increases as cells become more mature. In all cases colony expansion was independent of Young's modulus. The effect of Young's modulus on neuronal differentiation is thus dependent on the maturity of the starting population.

Acknowledgements

This work was supported by the Innovative Manufacturing Research Centre (IMRC) and Engineering and Physical Sciences Research Council (EPSRC), both based in the United Kingdom. The authors would like to gratefully acknowledge Zeinab Al-Rekabi for providing atomic force microscopy data for the GXG materials.

Appendix A. Supplementary data

Supplementary data associated with this article can be found, in the online version, at http://dx.doi.org/10.1016/j.actbio.2015.07.008.

References

[1] M.J. Evans, M.H. Kaufman, Establishment in culture of pluripotential cells from mouse embryos, Nature 292 (1981) 154–156.
[2] J.A. Thomson, J. Itskovitz-Eldor, S.S. Shapiro, M.A. Waknitz, J.J. Swiergel, V.S. Marshall, J.M. Jones, Embryonic stem cell lines derived from human blastocysts, Science 282 (5391) (1998) 1145–1147.
[3] A. Morizane, J.Y. Li, P. Brundin, From bench to bed: the potential of stem cells for the treatment of Parkinson's disease, Cell Tissue Res. 331 (1) (2008) 323–336.
[4] S. Lee, N. Lumelsky, L. Studer, J.M. Auerbach, R.D. McKay, Efficient generation of midbrain and hindbrain neurons from mouse embryonic stem cells, Nat. Biotechnol. 18 (2000) 675–679.
[5] S. Friling, M. Bergsland, S. Kjellander, Activation of Retinoid X Receptor increases dopamine cell survival in models in Parkinson's disease, BMC Neurosci. 10 (2009) 146.
[6] T. Vazin, R.S. Ashton, A. Conway, N.A. Rode, S.M. Lee, V. Bravo, et al., The effect of multivalent Sonic hedgehog on differentiation of human embryonic stem cells into dopaminergic and GABAergic neurons, Biomaterials 35 (3) (2014) 941–948.
[7] B. Soria, E. Roche, G. Berná, T. León-Quinto, J.A. Reig, F. Martín, Insulin-secreting cells derived from embryonic stem cells normalize glycemia in streptozotocin-induced diabetic mice, Diabetes 49 (2) (2000) 157–162.
[8] N. Lumelsky, O. Blondel, P. Laeng, I. Velasco, R. Ravin, R. McKay, Differentiation of embryonic stem cells to insulin-secreting structures similar to pancreatic islets, Science 292 (5520) (2001) 1389–1394.
[9] O. Naujok, S. Lenzen, Pluripotent stem cells for cell replacement therapy of diabetes, Dtsch. Med. Wochenschr. 137 (20) (2012) 1062–1066.
[10] I. Kehat, D. Kenyagin-Karsenti, M. Snir, H. Segev, M. Amit, A. Gepstein, et al., Human embryonic stem cells can differentiate into myocytes with structural and functional properties of cardiomyocytes, J. Clin. Invest. 108 (3) (2001) 407–414.
[11] I. Kehat, L. Khimovich, O. Caspi, A. Gepstein, R. Shofti, G. Arbel, et al., Electromechanical integration of cardiomyocytes derived from human embryonic stem cells, Nat. Biotechnol. 22 (2004) 1282–1289.
[12] M.V. Westfall, K.A. Pasyk, D.I. Yule, L.C. Samuelson, J.M. Metzger, Ultrastructure and cell-cell coupling of cardiac myocytes differentiating in embryonic stem cell cultures, Cell Motil. Cytoskeleton 36 (1) (1997) 43–54.
[13] J.Y. Min, Y. Yang, K.L. Converso, L. Liu, Q. Huang, J.P. Morgan, Y.F. Xiao, Transplantation of embryonic stem cells improved cardiac function in postinfarcted rats, J. Appl. Physiol. 92 (1) (2002) 288–296.
[14] S.J. Kattman, A.D. Witty, M. Gagliardi, N.C. Dubois, M. Niapour, A. Hotta, et al., Stage-specific optimization of activin/nodal and BMP signaling promotes cardiac differentiation of mouse and human pluripotent stem cell lines, Cell Stem Cell 8 (2) (2011) 228–240.
[15] Y. Choo, Discovery of small molecule regenerative drugs, in: C. Prescott, J. Polak (Eds.), The Delivery of Regenerative Medicines and Their Impact on Healthcare, CRC Press, Boca Raton, 2010, pp. 141–152.
[16] S. Abbasalizadeh, H. Baharvand, Technological progress and challenges towards cGMP manufacturing of human pluripotent stem cells based therapeutic products for allogeneic and autologous cell therapies, Biotechnol. Adv. 31 (2013) 1600–1623.
[17] F. Chowdhury, S. Na, D. Li, Y.C. Poh, T.S. Tanaka, F. Wang, N. Wang, Material properties of the cell dictate stress-induced spreading and differentiation in embryonic stem cells, Nat. Mater. 9 (1) (2010) 82–88.
[18] S. Stolberg, K.E. McCloskey, Can shear stress direct stem cell fate?, Biotechnol Prog. 25 (1) (2009) 10–19.
[19] A.J. Engler, S. Sen, H.L. Sweeney, D.E. Discher, Matrix elasticity directs stem cell lineage specification, Cell 126 (4) (2006) 677–689.
[20] J. Zoldan, E.D. Karagiannis, C.Y. Lee, D.G. Anderson, R. Langer, S. Levenberg, The influence of scaffold elasticity on germ layer specification of human embryonic stem cells, Biomaterials 32 (2011) 9612–9621.
[21] N. Eroshenko, R. Ramachandran, V.K. Yadavalli, R.R. Rao, Effect of substrate stiffness on early human embryonic stem cell differentiation, J. Biol. Eng. 7 (2013) 7.
[22] A.J. Engler, C. Carag-Krieger, C.P. Johnson, M. Raab, H.Y. Tang, D.W. Speicher, et al., Embryonic cardiomyocytes beat best on a matrix with heart-like elasticity: scar-like rigidity inhibits beating, J. Cell Sci. 121 (22) (2008) 3794–3802.
[23] R.J. Pelham, Y. Wang, Cell locomotion and focal adhesions are regulated by substrate flexibility, Proc. Natl. Acad. Sci. U.S.A. 94 (25) (1997) 13661–13665.
[24] A.J. Engler, M.A. Griffin, S. Sen, C.G. Bonnemann, H.L. Sweeney, D.E. Discher, Myotubes differentiate optimally on substrates with tissue-like stiffness: pathological implications for soft or stiff microenvironments, J. Cell Biol. 166 (6) (2004) 877–887.
[25] N.D. Evans, C. Minelli, E. Gentleman, V. LaPointe, S.N. Patankar, M. Kallivretaki, et al., Substrate stiffness affects early differentiation events in embryonic stem cells, Eur. Cell Mater. 18 (2009) 1–14.
[26] P.C. Georges, W.J. Miller, D.F. Meaney, E.S. Sawyer, P.A. Janmey, Matrices with compliance comparable to that of brain tissue select neuronal over glial growth in mixed cortical cultures, Biophys. J. 90 (8) (2006) 3012–3018.
[27] X. Jiang, P.C. Georges, B. Li, Y. Du, M.K. Kutzing, M.L. Previtera, et al., Cell growth in response to mechanical stiffness is affected by neuronal-astroglia interactions, Open Neurosci. J. 1 (2007) 7–14.
[28] M.L. Previtera, C.G. Langhammer, B.L. Firestein, Effects of substrate stiffness and cell density on primary hippocampal cultures, J. Biosci. Bioeng. 110 (4) (2010) 459–470.
[29] A. Banerjee, M. Arha, S. Choudhary, R.S. Ashton, S.R. Bhatia, D.V. Schaffer, R.S. Kane, The influence of hydrogel modulus on the proliferation and differentiation encapsulated neural stem cells, Biomaterials 30 (27) (2009) 4698–4699.
[30] K. Saha, A.J. Keung, E.F. Irwin, Y. Li, L. Little, D.V. Schaffer, K.E. Healy, Substrate modulus directs neural stem cell behavior, Biophys. J. 95 (9) (2008) 4426–4438.
[31] W.J. Tyler, The mechanobiology of brain function, Nat. Rev. Neurosci. 13 (12) (2012) 867–878.
[32] Q.-L. Ying, M. Stavridis, D. Griffiths, M. Li, A. Smith, Conversion of embryonic stem cells into neuroectodermal precursors in adherent monoculture, Nat. Biotechnol. 21 (2003) 183–186.
[33] L.A. Flanagan, Y.E. Ju, B. Marg, M. Osterfield, P.A. Janmey, Neurite branching on deformable substrates, NeuroReport 13 (18) (2002) 2411–2415.

[34] P. Mondragon-Teran, G.J. Lye, F.S. Veraitch, Lowering oxygen tension enhances the differentiation of mouse embryonic stem cells into neuronal cells, Biotechnol. Prog. 25 (5) (2009) 1480–1488.
[35] W. Hussain, N. Moens, F.S. Veraitch, D. Hernandez, C. Mason, G.J. Lye, Reproducible culture and differentiation of mouse embryonic stem cells using an automated microwell platform, Biochem. Eng. J. 77 (100) (2013) 246–257.
[36] S. Pachernegg, I. Joshi, E. Muth-Köhne, S. Pahl, Y. Münster, et al., Undifferentiated embryonic stem cells express ionotropic glutamate receptor mRNAs, Front. Cell. Neurosci. 7 (2013) 241.
[37] H. Ai, D.K. Mills, A.S. Jonathan, S.A. Jones, Gelatin-glutaraldehyde cross-linking on silicone rubber to increase endothelial cell adhesion and growth, In Vitro Cell. Dev. Biol. Anim. 38 (9) (2002) 487–492.
[38] Z. Al-Rekabi, A.E. Pelling, Cross talk between matrix elasticity and mechanical force regulates myoblast dynamics, Phys. Biol. 10 (6) (2013) 066003.
[39] Z. Al-Rekabi, K. Haase, Pelling AE Microtubules mediate changes in membrane cortical elasticity during contractile activation, Exp. Cell Res. 322 (1) (2014) 21–29.
[40] R. Matzke, K. Jacobson, M. Radmacher, Direct, high-resolution measurement of furrow stiffening during division of adherent cells, Nat. Cell Biol. 3 (6) (2001) 607–610.
[41] K. Miyake, N. Satomi, S. Sasaki, Elastic modulus of polystyrene film from near surface to bulk measured by nanoindentation using atomic force microscopy, Appl. Phys. Lett. 89 (031925) (2006) 1–2.
[42] J. Finne, Occurrence of unique polysialosyl carbohydrate units in glycoproteins of developing brain, J. Biol. Chem. 260 (1982) 1265–1270.
[43] U. Rutishauser, L. Landmesser, Polysialic acid in the vertebrate nervous system: a promoter of plasticity in cell–cell interactions, Trends Neurosci. 19 (10) (1996) 422–427.
[44] L. Gerrard, L. Rodgers, W. Cui, Differentiation of human embryonic stem cells to neural lineages in adherent culture by blocking bone morphogenetic protein signaling, Stem Cells 23 (2005) 1234–1241.
[45] S.-C. Zhang, M. Wernig, I.D. Duncan, O. Brüstle, J.A. Thomson, *In vitro* differentiation of transplantable neural precursors from human embryonic stem cells, Nat. Biotechnol. 19 (2001) 1129–1133.
[46] M.W. Pfaffl, A new mathematical model for relative quantification in real-time RT-PCR, Nucleic Acids Res. 29 (9) (2001) e:45.
[47] M. Kovacs, J. Tóth, C. Hetényi, A. Málnási-Csizmadia, J.R. Sellers, Mechanism of blebbistatin inhibition of myosin II, J. Biol. Chem. 279 (34) (2004) 35557–35563.
[48] M.J. De Brandbander, R.M.L. Van De Veire, F.E.M. Aerts, M. Borgers, P.A.J. Janssen, The effects of methyl [5-(2-thienylcarbonyl)-1H-benzimidazol-2-yl]carbamate, (R17934; NSC 238159), a new synthetic anti.tumoral drug interfering with microtubules, on mammalian cells cultured *in vitro*, J. Biol. Chem. 36 (3) (1976) 905–916.
[49] E. Spedden, J.D. White, E.N. Naumova, D.L. Kaplan, C. Staii, Elasticity maps of living neurons measured by combined fluorescence and atomic force microscopy, Biophys. J. 103 (5) (2012) 868–877.
[50] Y. Murayama, J. Mizuno, H. Kamakura, Y. Fueta, H. Nakamura, K. Akaishi, et al., Mouse zone pellucida dynamically changes its elasticity during oocyte maturation, fertilization and early embryo development, Hum. Cell 19 (4) (2006) 119–125.
[51] A. Pillarisetti, J.P. Desai, H. Ladjal, A. Schiffmacher, A. Ferreira, C.L. Keefer, Mechanical phenotyping of mouse embryonic stem cells: increase in stiffness with differentiation, Cell. Reprog. 13 (4) (2009) 1–10.
[52] M.H. Rosner, M.A. Viganao, K. Ozato, P.M. Timmons, F. Poirier, P.W. Rigby, L.M. Staudt, A POU-domain transcription factor in early stem cells and germ cells of the mammalian embryo, Nature 345 (1990) 686–692.
[53] H.R. Schöler, S. Ruppert, N. Suzuki, K. Chowdhury, P. Gruss, A new type of POU domain in germ line-specific protein Oct-4, Nature 344 (1990) 435–439.
[54] K. Okamoto, H. Okazawa, A. Okuda, M. Sakai, M. Muramatsu, H. Hamada, A novel octamer binding transcription factor is differentially expressed in mouse embryonic cells, Cell (1990) 461–472.
[55] F. Chowdhury, Y. Li, Y.C. Poh, T. Yokohama-Tamaki, N. Wang, T.S. Tanaka, Soft substrates promote homogeneous self-renewal of embryonic stem cells via downregulating cell-matrix tractions, PLoS One 5 (12) (2010) e15655.
[56] U. Lendahl, L.B. Zimmerman, R.D. McKay, CNS stem cells express a new class of intermediate filament protein, Cell 60 (4) (1990) 585–595.
[57] J.M. Encinas, G. Enikolopov, Identifying and quantitating neural stem and progenitor cells in the adult brain, Methods Cell Biol. 85 (2008) 243–272.
[58] A. Okuda, A. Fukushima, M. Nishimoto, A. Orimo, T. Yamagishi, Y. Nabeshima, et al., UTF1, a novel transcriptional coactivator expressed in pluripotent embryonic stem cells and extra-embryonic cells, EMBO J. 17 (7) (1998) 2019–2032.
[59] C. Hudson, D. Clements, R.V. Friday, D. Stott, H.R. Woodland, Xsox17alpha and -beta mediate endoderm formation in Xenopus, Cell 91 (1997) 397–405.
[60] O. Haub, M. Goldfarb, Expression of the fibroblast growth factor-5 gene in the mouse embryo, Development 112 (2) (1991) 397–406.
[61] D.G. Wilkinson, S. Bhatt, B.G. Herrmann, Expression pattern of the mouse T gene and its role in mesoderm formation, Nature 343 (6259) (1990) 657–659.
[62] N. Wang, J.D. Tytell, D.E. Ingber, Mechanotransduction at a distance: mechanically coupling the extracellular matrix with the nucleus, Nat. Rev. Mol. Cell Biol. 10 (2009) 75–82.
[63] G.M. Cooper, R. Hausman, The Cell: A Molecular Approach, 5th ed., Sinauer, Sunderland, MA, 2000. p504.
[64] D.E. Discher, P. Janmey, Y.L. Wang, Tissue cells feel and respond to the stiffness of their substrate, Science 310 (5751) (2005) 1139–1143.
[65] B.A. Danowski, Fibroblast contractility and actin organization are stimulated by microtubule inhibitors, J. Cell Sci. 93 (Pt 2) (1989) 255–266.
[66] T.J. Dennerll, H.C. Joshi, V.L. Steel, R.E. Buxbaum, S.R. Heidemann, Tension and compression in the cytoskeleton of PC-12 neurites. II: Quantitative measurements, J. Cell Biol. 107 (2) (1988) 665–674.
[67] C. Yang, M.W. Tibbitt, L. Basta, K.S. Anseth, Mechanical memory and dosing influence stem cell fate, Nat. Mater. 13 (2014) 645–652.
[68] K.F. Sullivan, Structure and utilization of tubulin isotypes, Ann. Rev. Cell. Biol. 4 (1998) 687–716.
[69] M.K. Lee, L.I. Rebhun, A. Frankfurter, Posttranslational modification of class III beta-tubulin, Proc. Natl. Acad. Sci. U.S.A. 87 (18) (1990) 7195–7199.
[70] K.F. Sullivan, D.W. Cleveland, Identification of conserved isotype-defining variable region sequences for four vertebrate beta tubulin polypeptide classes, Proc. Natl. Acad. Sci. U.S.A. 83 (12) (1986) 4327–4331.
[71] P.B. Molinoff, Biochemistry of catecholamines, Ann. Rev. Biochem. 40 (1971) 465–500.
[72] A. Bignami, L.F. Eng, D. Dahl, C.T. Uyeda, Localization of the glial fibrillary acidic protein in astrocytes by immunofluorescence, Brain Res. 43 (2) (1972) 429–435.
[73] A.L. Hemsley, D. Hernandez, C. Mason, A.E. Pelling, F.S. Veraitch, Precisely delivered nanomechanical forces induce blebbing in undifferentiated mouse embryonic stem cells, Cell Health Cytoskeleton 3 (2011) 23–34.
[74] Y.-C. Poh, F. Chowdhury, T.S. Tanaka, N. Wang, Embryonic stem cells do not stiffen on rigid substrates, Biophys. J. 99 (2) (2010) L19–L21.
[75] A.N. Ketene, P.C. Roberts, A.A. Shea, E.M. Schmelz, M. Agah, Actin filaments play a primary role for structural integrity and viscoelastic response in cells, Integr. Biol. (Camb.) 4 (2012) 540–549.
[76] K.A. Myers, K.T. Applegate, G. Danuser, R.S. Fischer, C.M. Waterman, Distinct ECM mechanosensing pathways regulate microtubule dynamics to control endothelial cell branching morphogenesis, J. Cell Biol. 192 (2) (2011) 321–334.
[77] R. Bernhardt, A.I. Matus, Light and electron microscopy studies of the distribution of microtubule-associated protein 2 in rat brain: a difference between the dendritic and axonal cytoskeletons, J. Comp. Neurol. 226 (1984) 203–219.
[78] C. Zhao, A. Tan, G. Pastorin, H.K. Ho, Nanomaterial scaffolds for stem cell proliferation and differentiation in tissue engineering, Biotechnol. Adv. 31 (5) (2013) 654–668.
[79] W. Ma, T. Tavakoli, E. Derby, Y. Serebryakova, M.S. Rao, M.P. Mattson, Cell-extracellular matrix interactions regulate neural differentiation of human embryonic stem cells, BMC Dev. Biol. 8 (2008) 90.
[80] S. Heydarkhan-Hagvall, J.M. Gluck, C. Delman, M. Jung, N. Ehsani, S. Full, R.J. Shemin, The effect of vitronectin on the differentiation of embryonic stem cells in a 3D culture system, Biomaterials 33 (2012) 2032–2040.
[81] J.G. Steele, G. Johnson, P.A. Underwood, Role of serum vitronectin and fibronectin in adhesion of fibroblasts following seeding onto tissue culture polystyrene, J. Biomed. Mater. Res. 26 (7) (1992) 861–864.
[82] B. Felding-Habermann, D.A. Cheresh, Vitronectin and its receptors, Current Opin. Cell Biol. 5 (5) (1993) 864–868.
[83] L.A. Flanagan, L.M. Rebaza, S. Derzic, P.H. Schwartz, E.S. Monuki, Regulation of human neural precursor cells by laminin and integrins, J. Neurosci. Res. 83 (2006) 845–856.
[84] W.M. Yu, H. Yu, Z.L. Chen, S. Strickland, Disruption of laminin in the peripheral nervous system impedes nonmyelinating Schwann cell development and impairs nociceptive sensory function, Glia 57 (8) (2009) 850–859.
[85] J. Candiello, S.S. Singh, K. Task, P.N. Kumta, I. Banerjee, Early differentiation patterning of mouse embryonic stem cells in response to variations in alginate substrate stiffness, J. Biol. Eng. 7 (1) (2013) 9.
[86] A.J. Keung, P. Asuri, S. Kumar, D.V. Schaffer, Soft microenvironments promote the early neurogenic differentiation but not self-renewal of human pluripotent stem cells, Integr. Biol. (Camb.) 4 (9) (2012) 1049–1058.
[87] M. Murakami, T. Ichisaka, M. Maeda, N. Oshiro, K. Hara, F. Edenhofer, et al., MTOR is essential for growth and proliferation in early mouse embryos and embryonic stem cells, Mol. Cell. Biol. 24 (15) (2004) 6710–6718.
[88] L. Magri, M. Cambiaghi, M. Cominelli, C. Alfaro-Cervello, M. Cursi, M. Pala, et al., Sustained activation of mTOR pathway in embryonic neural stem cells leads to development of tuberous sclerosis complex-associated lesions, Cell Stem Cell 9 (5) (2011) 447–462.
[89] S.M. Brouxhon, S. Kyrkanides, X. Teng, M. Athar, S. Ghazizadeh, M. Simon, et al., Soluble E-cadherin: a critical oncogene modulating receptor tyrosine kinases, MAPK and PI3K/Akt/mTOR signalling, Oncogene 33 (2) (2014) 225–235.
[90] C.R. Kothapalli, R.D. Kamm, 3D matrix microenvironment for targeted differentiation of embryonic stem cells into neural and glial lineages, Biomaterials 34 (25) (2013) 5995–6007.
[91] S. Musah, P.J. Wrighton, Y. Zaltsman, X. Zhong, S. Zorn, et al., Substratum-induced differentiation of human pluripotent stem cells reveals the coactivator YAP is a potent regulator of neuronal specification, Proc. Natl. Acad. Sci. U.S.A. 111 (38) (2014) 13805–13810.
[92] M.L. Previtera, M. Hui, D. Verma, A.J. Shahin, R. Schloss, N.A. Langrana, The effects of substrate elastic modulus on neural precursor cell behavior, Ann. Biomed. Eng. 41 (6) (2013) 1193–1207.
[93] K.M. McAndrews, M.J. Kim, T.Y. Lam, D.J. McGrail, M.R. Dawson, Architectural and mechanical cues direct mesenchymal stem cell interactions with cross-linked gelatin scaffolds, Tissue Eng. Part A (2014) (Epub ahead of print).
[94] J.W. Fawcett, R.A. Asher, The glial scar and central nervous system repair, Brain Res. Bull. 49 (6) (1999) 377–391.